Residual Interference and Wind-Tunnel Wall Adaptation

M. Mokry*
National Research Council Canada, Ottawa, Ontario, Canada

This paper reviews a linear theory of residual interference in adaptive wall wind tunnels. One-variable, two-variable, and interface discontinuity methods are analyzed. Their autocorrective properties and connections with some well-known adaptation criteria, such as the single-step convergence formulas and the functional relationships for unconfined flow, are discussed. A simple procedure for the evaluation of residual interference by the two-variable method in a two-dimensional test section is described and applied to the NASA Langley Transonic Cryogenic Wind Tunnel and the ONERA/CERT T2 adaptive wall wind-tunnel data.

Nomenclature

C = test section contour (interface)
C_N = normal force coefficient
C_p = boundary pressure coefficient
f = density function of Cauchy-type integral
G = source singularity
h = distance of parallel boundaries (interfaces)
i = $\sqrt{-1}$
Im = imaginary part
M = Mach number
n = outward normal direction with respect to S
q = modulus of disturbance velocity
r = position vector, (x',y,z)
Rc = Reynolds number based on chord
Re = real part
s = circumferential coordinate on C
S = test section boundary (interface)
u,v,w = disturbance velocity components
U = streamwise component of velocity
w = complex disturbance velocity, $u - iv$
x,y,z = Cartesian coordinates in physical plane
x',y,z = Cartesian coordinates in transformed plane
z = complex coordinate in transformed plane, $x' + iy$
α = angle of incidence
β = $\sqrt{1 - M_\infty^2}$
γ = vortex density
δ = Dirac's delta function
Δ = wall interference correction
ϑ = increment (error)
κ = ratio of specific heats, 1.4
σ = source density
ϕ = disturbance velocity potential
Ω = vortex singularity
∇ = nabla vector

Subscripts

j = line segment number
m = model-induced
n = normal component
t = tangential component
w = wall-induced
0 = observation point
∞ = (upstream) reference

Superscripts

$*$ = critical value
$\sim$ = exterior (fictitious) flow

Presented as Paper 89-0147 at the AIAA 27th Aerospace Sciences Meeting, Reno, NV, Jan. 9–12, 1989; received Feb. 7, 1989; revision received Sept. 18, 1989.

*Senior Research Officer, High Speed Aerodynamics Laboratory, Institute for Aerospace Research. Member AIAA.

I. Introduction

MEASURED flow variables near the test section boundaries, used to guide adjustments of the walls in adaptive wind tunnels, can also be used to quantify the residual interference. Because of a finite number of wall control devices (jacks, plenum compartments), the finite test section length, and the approximation character of adaptation algorithms, the unconfined flow conditions are not likely to be attained even in the "fully" adapted stage.[1,2] Assessment of residual interference is of particular importance not only for two-dimensional (2-D) testing, but also for three-dimensional (3-D) testing in test sections with two adaptive walls, where only a partial adaptation is possible.[3–5]

The linear techniques for the evaluation of residual wall interference are essentially the same as those used to assess the corrections in conventional, nonadaptive wind tunnels. Depending upon the number of flow variables measured, we speak of one- or two-variable methods[6]; in two dimensions also of Schwarz- or Cauchy-type methods.[7]

The one-variable methods, as the name indicates, require that one flow variable, usually the pressure, be measured at the test section boundary. In addition, model-induced perturbations must be estimated along the (far-field) boundary.

The two-variable methods use measurements of static pressure and normal velocity at the test section boundary but do not require any model representation. This is clearly an advantage for adaptive wall test sections, which are often relatively small with respect to the test model, and for the variety of complex flows commonly encountered in wind-tunnel testing. The method[8] utilizing measurement of a single flow variable along a double boundary falls in the same category, as no model representation is needed to evaluate the corrections.

The interface discontinuity method, also described, is a "genuine" residual interference assessment technique. It is specific to wall adaptation schemes utilizing measurement of two flow variables on the inner side of an interface (wind-tunnel flow boundary) and computations of the fictitious, infinite flow on the outer side.

II. Linear Flow Analysis

Provided that the adaptive walls introduce only minor disturbances to the far field of the test model, the linearization of the potential equation near the walls is justifiable as long as the walls remain subcritical.

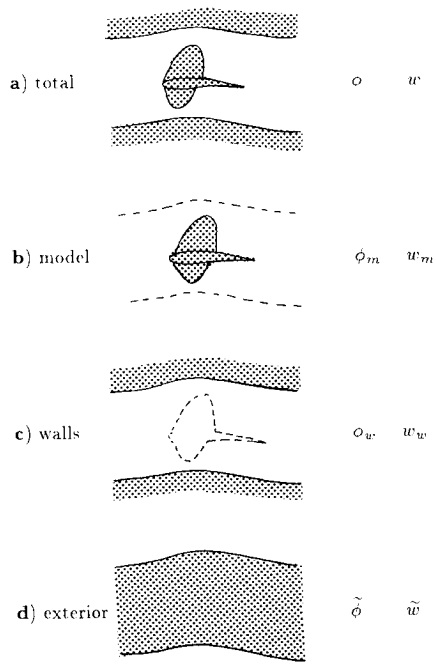

Fig. 1 Linearized flow regions

The governing equation for the disturbance velocity potential is

$$\beta^2 \frac{\partial^2 \phi}{\partial x^2} + \frac{\partial^2 \phi}{\partial y^2} + \frac{\partial^2 \phi}{\partial z^2} = 0 \tag{1}$$

where $M_\infty < 1$ is the stream Mach number.

The scaling of the streamwise coordinate

$$x' = \frac{x}{\beta} \tag{2}$$

reduces Eq. (1) to Laplace's equation, $\nabla^2 \phi = 0$.

The linear flow region where ϕ satisfies Eq. (1) is shown schematically in Fig. 1a. It excludes the volume occupied by the test model, the viscous and transonic flow regions, and the wind-tunnel exterior (the cross-hatched regions). The outer bounding surface, enclosing the test model, is required to lie entirely within the linear flow region, off the viscous or nonisentropic flow at the walls.

Using the principle of linear superposition, the disturbance velocity potential is split as[9]

$$\phi = \phi_m + \phi_w \tag{3}$$

where ϕ_m is that due to the model in free air and ϕ_w is that due to wall interference.

The model potential ϕ_m satisfies Eq. (1) in the infinite space outside the model and the adjacent nonlinear flow regions; see Fig. 1b.

The wall interference potential ϕ_w is assumed to satisfy Eq. (1) in the whole test section interior, including the model and its nonlinear flow regions, as indicated in Fig. 1c.

This assignment of the singular and nonsingular parts as the effects of the model and the walls, respectively, is consistent with the concept of the Green's function for the Laplace operator. Understandably, it is rigorous for a point disturbance (source), but only approximate for a finite-size model.

The derivatives of ϕ_w are interpreted as disturbances to stream velocity components. They are usually evaluated at the model reference station or as averages over the model and interpreted as global corrections to stream Mach number[10]

$$\Delta M_\infty = \left(1 + \frac{\kappa - 1}{2} M_\infty^2\right) M_\infty \frac{\partial \phi_w}{\partial x} \tag{4}$$

and to flow angles (in radians)

$$\Delta \alpha_y = \frac{\partial \phi_w}{\partial y} \quad \text{and} \quad \Delta \alpha_z = \frac{\partial \phi_w}{\partial z} \tag{5}$$

From the spatial variations of these corrections over the model, additional streamline curvature and buoyancy effects on model force data can be determined.

The evaluation of the local corrections to model surface pressure coefficient or Mach number M is an approach more rigorous, but of course less practical, from the point of view of the interpretation of the wind-tunnel data in terms of free-flight conditions. Unlike the conventional, passive walls, the adaptive walls can, in principle, be adjusted to minimize the wall-induced velocity gradients to render the test data correctable in terms of the global corrections to stream parameters even in very extreme conditions (large models with respect to the test section size, high angle-of-attack tests, etc.).

In connection with adaptive wall wind tunnels, another type of the disturbance velocity potential is of importance: that corresponding to the "fictitious" flow outside the interface. The potential, denoted here by the symbol $\tilde{\phi}$, satisfies Eq. (1) in the infinite exterior region, outside the shaded area in Fig. 3d.

A. One-Variable Method

The method of Capelier, et al.[11] is one of the most widely used techniques for the post-test assessment of subsonic wall interference in wind tunnels with perforated walls. It retains the essential features of the theoretical wall interference approach[9] but replaces the idealized wind-tunnel boundary conditions by the linearized "pressure" boundary condition

$$\frac{\partial \phi}{\partial x} = -\frac{1}{2} C_p \tag{6}$$

The control surface along which the pressure is measured is required to be some distance away from the walls, where the disturbances from the individual holes (perforations) are sufficiently smeared out. The most common approach is to use pressure rails or pipes, attached directly to the walls.

The application of the method to test sections with slotted walls is more problematic as the discrete wall disturbances decay at larger distances from the walls. The pressures measured directly on slat surfaces, on the other hand, are not necessarily representative of the averaged static pressures near the walls.

The streamwise component of wall interference velocity

$$u_w = \frac{\partial \phi_w}{\partial x} \tag{7}$$

satisfies inside the test section

$$\beta^2 \frac{\partial^2 u_w}{\partial x^2} + \frac{\partial^2 u_w}{\partial y^2} + \frac{\partial^2 u_w}{\partial z^2} = 0 \tag{8}$$

and is obtained from the boundary values

$$u_w = -\frac{1}{2} C_p - \frac{\partial \phi_m}{\partial x} \tag{9}$$

as a solution of the interior Dirichlet problem. The transverse velocity components

$$v_w = \frac{\partial \phi_w}{\partial y} \quad \text{and} \quad w_w = \frac{\partial \phi_w}{\partial z} \tag{10}$$

are obtained from u_w by integrating the irrotational flow conditions

$$\frac{\partial v_w}{\partial x} = \frac{\partial u_w}{\partial y} \quad \text{and} \quad \frac{\partial w_w}{\partial x} = \frac{\partial u_w}{\partial z} \tag{11}$$

along a path from the upstream end of the test section, where the flow direction is expected to be known.

The Dirichlet problem for Laplace's equation is one of the best-explored problems in mathematical physics, and there are a large number of methods available to solve it numerically. A natural approach is to solve the problem in terms of the double-layer potential,[12] leading to a doublet panel method.[13] For simpler geometries, closed-form solutions are obtainable using integral transforms[11] or the Fourier method.[14-16]

The complex-variable treatment of the 2-D case leads, as pointed out by Smith,[7] to the Schwarz problem. It consists of determining an analytic function inside a domain from its defined real part on the boundary. Theory[17] shows that the integration of Cauchy-Riemann equations (irrotational-flow conditions) introduces an unknown imaginary constant that needs to be specified in order to make the solution unique (specification of the upstream flow angle).

The accuracy of the one-variable method depends greatly on the accuracy with which the free air potential ϕ_m can be estimated on the control surfaces.[18,19] Since the far field of ϕ_m is normally evaluated using the measured model loading, which is subject to wall interference, the prediction tends to be more exact near a fully adapted stage. However, with respect to the size of the model, the adaptive test sections are usually much narrower than the conventional ones, so that the representation of flow near the walls in terms of the model far field may not be that satisfactory after all.

Another source of inaccuracy, which is common to all residual interference methods based on boundary measurements, is the finite length of the test section and sparseness of the experimental pressure data. The boundary values of u_w need to be interpolated or extrapolated over a complete boundary (closed or infinite) in order to make the Dirichlet problem soluble. The adaptive test sections, which are typically longer than the conventional ones, will have a slight advantage in this regard.

The one-variable method can be used to monitor the reduction of wall interference corrections in the course of adaptation but can also be incorporated into the adaptation algorithm.[20] The necessary condition for flow to be interference-free (unconfined) is that the boundary values of u_w vanish:

$$u_w \equiv 0 \quad \text{on} \quad S \tag{12}$$

Compensation for errors of the reference velocity or pressure,[11] also called the autocorrective property[19] or autoconvergence,[21] is an important feature of the method. It may be described as follows: If the error of the (upstream) reference velocity U_∞ is ϑU_∞, then the perturbation velocities $U - U_\infty$ on the boundary will be offset by $-\vartheta U_\infty$. Since

$$\vartheta u_w = -\vartheta U_\infty / U_\infty = \text{const}$$

is also a solution of Eq. (8), the incremental velocity correction, being of equal magnitude but opposite sign to the reference velocity error, restores U_∞ as the reference velocity.

Admittedly, if the perturbation velocities are obtained from the measured pressures using the linearized Bernoulli theorem, Eq. (6), the autocorrective property is valid only as the first order approximation.[21]

Besides compensating for genuine reference velocity errors, the autocorrective principle is also indispensable for establishing the correspondence between U_∞ based on plenum pressure and the actual stream velocity in ventilated test sections.[15]

B. Two-Variable Method

Measurement of the static pressure and normal velocity distributions along the control surface, which is a prerequisite for wall adaptation, opens the possibility of evaluating subsonic wall interference without model representation. Incidentally, this feature also allows accounting for the presence of the model support system (sting, strut) but only as far as the indirect, wall-induced effect on the model is concerned.

The method is ideally suited for test sections with flexible walls, where the normal component of disturbance velocity can be obtained directly from the shape of the wall or, more accurately, from its boundary-layer displaced stream surface. For ventilated walls the Calspan pipes or laser Doppler velocimetry provide possible means of measuring two components of velocity. However, because of the disturbed flow environment of the walls, such measurements still pose difficult technical problems.

The first successful evaluation of the 2-D interference flowfield from two flow variables measured at the control surface was reported by Lo.[22] Both numerical demonstration and experimental verification are given in the same paper. The method uses the Fourier transform solution[23] for linearized subsonic flow past a nonlifting airfoil. A more straightforward Cauchy's integral approach to the two-variable method was subsequently described by Kraft and Dahm,[24] Smith,[7] and Amecke.[25] An extension to 3-D flows, based on Green's theorem, is from the work of Ashill and Weeks.[26]

To describe the method using the latter approach, we introduce the position vectors of an interior point and a boundary point,

$$\boldsymbol{r}_0 = (x'_0, y_0, z_0) \quad \text{and} \quad \boldsymbol{r} = (x', y, z) \tag{13}$$

Further, denote by

$$G(\boldsymbol{r}_0, \boldsymbol{r}) = -\frac{1}{4\pi |\boldsymbol{r}_0 - \boldsymbol{r}|} \tag{14}$$

the fundamental solution (unit-strength source), satisfying

$$\nabla^2 G(\boldsymbol{r}_0, \boldsymbol{r}) = \delta(\boldsymbol{r}_0 - \boldsymbol{r}) \tag{15}$$

where δ is the 3-D Dirac delta function.

Green's second identity gives for ϕ_w harmonic in the test section interior

$$\phi_w(\boldsymbol{r}_0) = \int\int_S \left[\phi_w(\boldsymbol{r}) \frac{\partial G(\boldsymbol{r}_0, \boldsymbol{r})}{\partial n} - G(\boldsymbol{r}_0, \boldsymbol{r}) \frac{\partial \phi_w(\boldsymbol{r})}{\partial n} \right] \mathrm{d}S$$

and for ϕ_m harmonic in the test section exterior

$$0 = \int\int_S \left[\phi_m(\boldsymbol{r}) \frac{\partial G(\boldsymbol{r}_0, \boldsymbol{r})}{\partial n} - G(\boldsymbol{r}_0, \boldsymbol{r}) \frac{\partial \phi_m(\boldsymbol{r})}{\partial n} \right] \mathrm{d}S$$

The differential and integral operations are taken with respect to the unsubscripted coordinates in the transformed space (x', y, z) and $\partial/\partial n$ is the derivative in the direction of the exterior normal to the boundary S.

Adding the preceding formulas and eliminating ϕ_m from Eq. (3), we obtain the correction formula[26]:

$$\phi_w(\boldsymbol{r}_0) = \int\int_S \left[\phi(\boldsymbol{r}) \frac{\partial G(\boldsymbol{r}_0, \boldsymbol{r})}{\partial n} - G(\boldsymbol{r}_0, \boldsymbol{r}) \frac{\partial \phi(\boldsymbol{r})}{\partial n} \right] \mathrm{d}S \tag{16}$$

It expresses the wall interference potential at a given interior point $\boldsymbol{r}_0$ in terms of the boundary values of the (total) disturbance velocity potential and its normal derivative.

Considering the entire space, Eq. (16) describes a sectionally harmonic function ϕ_w having a jump discontinuity of magnitude ϕ across the surface S. This differs from the more conventional representation of the wall interference potential

by external singularities (images), where ϕ_w is continuous across S and harmonic everywhere except at the singular points. Of course, inside the test section both representations are equivalent.

Physically, the integral (16) can be interpreted as a surface distribution of doublets

$$\frac{\partial G(\boldsymbol{r}_0,\boldsymbol{r})}{\partial n} \quad \text{with density} \quad \phi(\boldsymbol{r})$$

and a surface distribution of sources

$$G(\boldsymbol{r}_0,\boldsymbol{r}) \quad \text{with density} \quad -\frac{\partial \phi(\boldsymbol{r})}{\partial n}$$

The normal component of disturbance velocity $\partial\phi/\partial n$ can be measured directly, whereas the potential ϕ must be evaluated by the streamwise integration of the measured pressure coefficient, Eq. (6).

For a cylindrical boundary parallel to the x axis the streamwise integration in Eq. (16) can be done by parts, converting the surface distribution of doublets into a surface distribution of horseshoe vortices[27]

$$\Omega(\boldsymbol{r}_0,\boldsymbol{r}) = \int_{x'}^{\infty} \frac{\partial G(\boldsymbol{r}_0,\boldsymbol{r})}{\partial n}\,\mathrm{d}x' \tag{17}$$

with density

$$\frac{\partial \phi(\boldsymbol{r})}{\partial x'} = -\frac{\beta}{2} C_p(\boldsymbol{r})$$

that can be measured directly. The isolated integration terms vanish by the virtue of

$$\Omega(\boldsymbol{r}_0,\boldsymbol{r}) \to \quad \text{as} \quad x' \to \infty$$

and

$$\phi(\boldsymbol{r}) \to 0 \quad \text{as} \quad x' \to -\infty$$

The autocorrective property applies[19] and is easy to verify. Denoting by ϑU_∞ the error of the reference velocity, the boundary values of the disturbance velocity potential ϕ will be subject to the (systematic) error

$$\vartheta\phi(\boldsymbol{r}) = -\frac{\vartheta U_\infty}{U_\infty} x$$

The corresponding increment $\vartheta\phi_w$ of the wall interference potential is obtained by substituting $\vartheta\phi \to \phi$ into Eq. (16). Converting the surface integral into the volume integral, using Eq. (15) and the fact that $\nabla^2\vartheta\phi = 0$, it follows that

$$\vartheta\phi_w(\boldsymbol{r}_0) = \iiint_V [\vartheta\phi(\boldsymbol{r})\nabla^2 G(\boldsymbol{r}_0,\boldsymbol{r}) - G(\boldsymbol{r}_0,\boldsymbol{r})\nabla^2\vartheta\phi(\boldsymbol{r})]\,\mathrm{d}V$$
$$= \vartheta\phi(\boldsymbol{r}_0)$$

This result shows again that the correction compensates for the reference velocity error.

Turning back to Eq. (16) and taking the limit as $\boldsymbol{r}_0$ becomes a point of a smooth surface element (facing the interior flow), we obtain

$$\phi_w(\boldsymbol{r}_0) = \frac{1}{2}\phi(\boldsymbol{r}_0) + \iint_S \left[\phi(\boldsymbol{r})\frac{\partial G(\boldsymbol{r}_0,\boldsymbol{r})}{\partial n} - G(\boldsymbol{r}_0,\boldsymbol{r})\frac{\partial \phi(\boldsymbol{r})}{\partial n}\right]\mathrm{d}S, \quad \boldsymbol{r}_0 \in S \tag{18}$$

The integral is to be interpreted as a principal value in the sense that a small circular neighborhood of the (singular) point $\boldsymbol{r}_0$ is removed from the surface S for the doublet integral; its contribution has already been accounted for by the isolated term $\frac{1}{2}\phi(\boldsymbol{r}_0)$. There is no ambiguity concerning the source integral, as the contribution of a small circular element around the point $\boldsymbol{r}_0$ is zero.

Further, eliminating ϕ_w from Eqs. (3) and (18), it follows that[4]

$$\phi_m(\boldsymbol{r}_0) = \frac{1}{2}\phi(\boldsymbol{r}_0) - \iint_S \left[\phi(\boldsymbol{r})\frac{\partial G(\boldsymbol{r}_0,\boldsymbol{r})}{\partial n} - G(\boldsymbol{r}_0,\boldsymbol{r})\frac{\partial \phi(\boldsymbol{r})}{\partial n}\right]\mathrm{d}S, \quad \boldsymbol{r}_0 \in S \tag{19}$$

This formula determines the boundary value of the free air potential ϕ_m from the measured boundary values of ϕ and $\partial\phi/\partial n$. Provided that the differences between the boundary values of ϕ and ϕ_m are small, it may be possible to achieve $\phi = \phi_m$ in a single adjustment of the walls. Equation (19) will then play the role of a single-step convergence formula.[23]

Alternative formulations of the corrections based on Green's theorem are given in Refs. 28 and 29; comparisons and accuracy aspects are discussed in Ref. 30. In the absence of model representation, the sparseness of boundary data and incomplete test section boundary remain as a major source of inaccuracy.

Using a physical argument, the existence of unconfined flow conditions for 3-D flow in the form of functional relationships between two flow variables on the bounding surface was stated by Sears.[1] For linear flow, the relationship is, in fact, quite simple: setting $\phi_w = 0$ in Eq. (18) or $\phi_m = \phi$ in Eq. (19), we obtain

$$\frac{1}{2}\phi(\boldsymbol{r}_0) = -\iint_S \left[\phi(\boldsymbol{r})\frac{\partial G(\boldsymbol{r}_0,\boldsymbol{r})}{\partial n} - G(\boldsymbol{r}_0,\boldsymbol{r})\frac{\partial \phi(\boldsymbol{r})}{\partial n}\right]\mathrm{d}S, \quad \boldsymbol{r}_0 \in S \tag{20}$$

The formula determines the value of ϕ at a given surface point $\boldsymbol{r}_0$ in terms of the values of ϕ and $\partial\phi/\partial n$ over the whole surface S. If it holds true for all surface points $\boldsymbol{r}_0$, then the flow inside the test section is interference-free (unconfined).

The descent to two dimensions is accomplished by putting

$$\boldsymbol{r}_0 = (x'_0, y_0), \qquad \boldsymbol{r} = (x', y), \qquad G(\boldsymbol{r}_0,\boldsymbol{r}) = \frac{1}{2\pi}\ell n|\boldsymbol{r}_0 - \boldsymbol{r}|$$

and replacing the surface integrals by contour integrals. Further details of this approach are given by Labrujère.[29]

However, more readily applicable results can be obtained using Cauchy's integral formula. To illustrate the latter approach, we introduce the complex coordinate

$$z = x' + iy = \frac{x}{\beta} + iy \tag{21}$$

and the complex disturbance velocity

$$w(z) = \beta u(x,y) - iv(x,y) = \beta\frac{\partial\phi}{\partial x}(x,y) - i\frac{\partial\phi}{\partial y}(x,y) \tag{22}$$

In accordance with Eq. (3), the complex disturbance velocity is decomposed as

$$w(z) = w_m(z) + w_w(z) \tag{23}$$

where w_w is analytic in the test section interior, and w_m is analytic in the test section exterior (see Figs. 1b and 1c). Applying the Cauchy integral formula to a counterclockwise oriented contour C, we obtain for an interior point z_0

$$w_w(z_0) = \frac{1}{2\pi i}\int_C \frac{w_w(z)}{z - z_0}\,\mathrm{d}z$$

and

$$0 = \frac{1}{2\pi i}\int_C \frac{w_m(z)}{z - z_0}\,dz$$

Adding the integrals and eliminating w_m from Eq. (23), we obtain the correction formula[7]:

$$w_w(z_0) = \frac{1}{2\pi i}\int_C \frac{w(z)}{z - z_0}\,dz \tag{24}$$

expressing the wall interference velocity in terms of boundary value of the (total) disturbance velocity. Using Eq. (22), the components of the wall interference velocity are obtained as

$$u_w(x_0,y_0) = \frac{1}{\beta}\,\mathrm{Re}[w_w(z_0)] \tag{25a}$$

$$v_w(x_0,y_0) = -\mathrm{Im}[w_w(z_0)] \tag{25b}$$

To evaluate the Cauchy-type integral [Eq. (24)] along a curved contour, the present paper uses a trapezoidal rule described in Appendix A. A sample of wall deflections and wall pressures from the tests[31] of the 9-in. chord CAST 10-2/DOA 2 airfoil in the 13-in. flexible-wall test section of the Langley Transonic Cryogenic Wind Tunnel (TCT) is shown in Fig. 2. The wall pressure distribution at the stream Mach number of 0.700 is well below the critical value ($C_p^* = -0.779$). The downstream end of the integration contour was placed so as to eliminate the three most downstream pressure points diverging from the undisturbed flow level (diffuser effect). The distribution of residual corrections along the wind-tunnel axis, evaluated from Eqs. (24) and (25), is shown by solid lines in Fig. 3. The flow in the test section is not interference free, but, considering the size of the model with respect to the test section, the corrections are certainly small.

The broken lines in Fig. 3 are the corrections corresponding to the stream Mach number arbitrarily changed from 0.700 to 0.695, with the input pressure coefficients of Fig. 2 adjusted accordingly. We note that the resultant Mach number correction curve, corresponding to $M_\infty = 0.695$ is displaced approximately by 0.005 in the positive direction, confirming the validity of the autocorrective principle. The angle of attack correction, as expected, is not greatly affected by the change of the reference Mach number.

Considering the entire complex plane, Eq. (24) describes a sectionally analytic function w_w having a jump discontinuity w across the contour C. Again, this is in contrast with the conventional representation of the complex interference velocity by external poles, allowing w_w to the continued analytically across C, but only up to the location of the poles.

The physical meaning of the Cauchy-type integral [Eq. (24)] becomes more apparent when recast as

$$w_w(z_0) = \int_C \left[\frac{i\gamma(z)}{2\pi(z_0 - z)} + \frac{\sigma(z)}{2\pi(z_0 - z)}\right] ds \tag{26}$$

where $ds = |dz|$ is the length of the counterclockwise-oriented contour element.

In this form, it represents a line distribution of vortices with density

$$\gamma(z) = \mathrm{Re}\left[w(z)\frac{dz}{|dz|}\right] = q_t(z) \tag{27}$$

and a line distribution of sources with density

$$\sigma(z) = -\mathrm{Im}\left[w(z)\frac{dz}{|dz|}\right] = -q_n(z) \tag{28}$$

where q_t is the tangential component of disturbance velocity (positive in the counterclockwise direction), and q_n is the normal component of disturbance velocity (positive in the

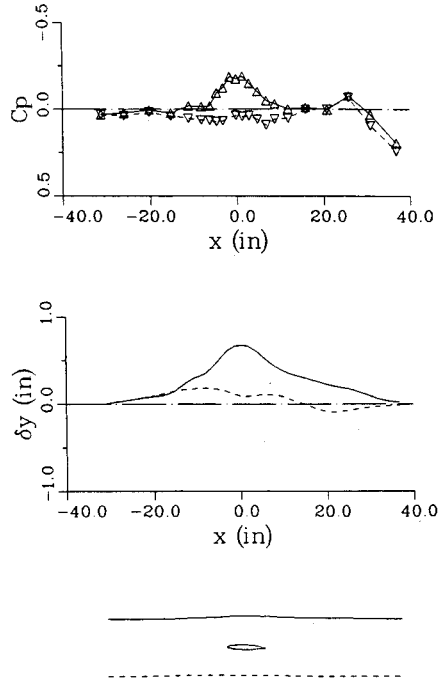

Fig. 2 Wall pressure coefficients and deflections; 9-in. chord CAST 10 airfoil in the 13-in. × 13-in. test section of NASA TCT, $M_\infty = 0.700$, $\alpha = 1.20$ deg, $C_N = 0.50$, $Rc = 30 \times 10^6$.

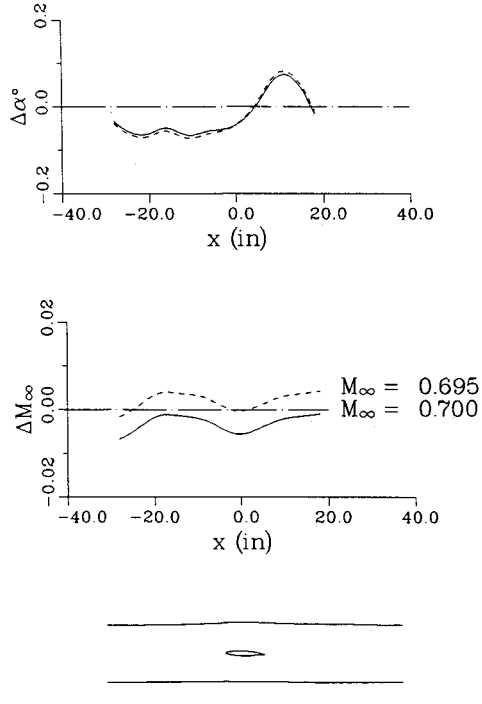

Fig. 3 Residual corrections along test section axis, evaluated by two-variable method from data of Fig. 2.

direction of the outward normal). The correspondence with Green's theorem approach is evident.

The correction formula [Eq. (24)] is closely related to wall adaptation criteria for the 2-D testing. In the limiting process, as z_0 becomes a point on a smooth segment of the contour C, we obtain

$$w_w(z_0) = \frac{1}{2} w(z_0) + \frac{1}{2\pi i} \int_C \frac{w(z)}{z - z_0} \, dz, \quad z_0 \in C \tag{29}$$

where the (singular) integral is to be interpreted as Cauchy's principal value.

Substituting Eq. (29) into Eq. (23), we find

$$w_m(z_0) = \frac{1}{2} w(z_0) - \frac{1}{2\pi i} \int_C \frac{w(z)}{z - z_0} \, dz, \quad z_0 \in C \tag{30}$$

This formula determines the boundary value of w_m of the complex disturbance velocity due to the model in free air, in terms of the measured values w on the boundary. In fact, it can be used as the near-field boundary condition for the computation of flow past an airfoil in free air.[32]

This result shows again that the model representation in the two-variable method is, in theory, superfluous. However, for incomplete boundary data, an independently estimated far field of w_m may facilitate extrapolations towards far upstream and downstream ends of the test section.

Equation (30) may also be used as the 2-D single-step convergence formula. For straight-line boundaries at $y = \pm h/2$, we obtain in terms of disturbance velocity components

$$\begin{aligned} u_m\left(x_0, \pm\frac{h}{2}\right) &= \frac{1}{2} u\left(x_0, \pm\frac{h}{2}\right) \mp \frac{1}{2\pi\beta} \int_{-\infty}^{\infty} \frac{v\left(x, \pm\frac{h}{2}\right)}{x - x_0} \, dx \\ &\quad - \frac{\beta h}{2\pi} \int_{-\infty}^{\infty} \frac{u\left(x, \mp\frac{h}{2}\right)}{(x - x_0)^2 + (\beta h)^2} \, dx \\ &\quad \pm \frac{1}{2\pi\beta} \int_{-\infty}^{\infty} \frac{(x - x_0)\, v\left(x, \mp\frac{h}{2}\right)}{(x - x_0)^2 + (\beta h)^2} \, dx \end{aligned} \tag{31a}$$

$$\begin{aligned} v_m\left(x_0, \pm\frac{h}{2}\right) &= \frac{1}{2} v\left(x_0, \pm\frac{h}{2}\right) \pm \frac{\beta}{2\pi} \int_{-\infty}^{\infty} \frac{u\left(x, \pm\frac{h}{2}\right)}{x - x_0} \, dx \\ &\quad - \frac{\beta h}{2\pi} \int_{-\infty}^{\infty} \frac{v\left(x, \mp\frac{h}{2}\right)}{(x - x_0)^2 + (\beta h^2)} \, dx \\ &\quad \mp \frac{\beta}{2\pi} \int_{-\infty}^{\infty} \frac{(x - x_0)\, u\left(x, \mp\frac{h}{2}\right)}{(x - x_0)^2 + (\beta h)^2} \, dx \end{aligned} \tag{31b}$$

Similar single-step convergence formulas were first obtained by Lo and Kraft,[23] by solving a problem of the optimum iterative wall adaptation for a linearized flow past a symmetric, nonlifting airfoil. Lo and Sickles[33] have extended the analysis to lifting airfoils and to axisymmetric bodies (in an axisymmetric wind tunnel). Kraft and Dahm[24] completed the analysis by developing both a single-step adaptation method and a two-variable residual wall-interference calculation procedure. Equations (31) are valid for the general case including lifting and thickness effects, as is reasonable to expect from a two-variable method.

From the point of view of high-productivity testing, it is of great importance that predictive wall contouring and single-step schemes provide low residual interference in early stages of adaptation. An example of residual corrections corresponding to four iterative adaptation steps of the ONERA/CERT T2 flexible walled test section is shown in Fig. 4. The streamwise distributions of corrections along the straight line passing through the model are evaluated by the two-variable method using the experimental data.[34] The CAST 7 airfoil was placed asymmetrically with respect to the test section, in order to keep the walls subcritical at higher stream Mach numbers and positive model incidences and, also, to stay within the flexing limits of the facility.[35]

Residual interference corrections corresponding to the first three iterations are plotted (regardless of order) by broken lines and the final, fourth iteration, by the solid line. It is seen that the differences between the iterations are quite small, which is an indication that the practical limits of wall adaptation were reached from the very start of the iterative process. The level of residual corrections is comparable to those shown earlier in Fig. 3 for the TCT test section.

Setting $w_w = 0$ in Eq. (29) or $w_m = w$ in Eq. (30), we obtain the unconfined flow condition

$$\frac{1}{2} w(z_0) = -\frac{1}{2\pi i} \int_C \frac{w(z)}{z - z_0} \, dz, \quad z_0 \in C \tag{32}$$

in terms of the complex disturbance velocity on the boundary. The factor 1/2 was left uncancelled to emphasize the connection with the 3-D case, Eq. (20).

Considering straight-line boundaries at $y = \pm h/2$, we obtain in terms of disturbance velocity components

$$u\left(x_0, \pm\frac{h}{2}\right) = \mp \frac{1}{\beta\pi} \int_{-\infty}^{\infty} \frac{v\left(x, \pm\frac{h}{2}\right)}{x - x_0} \, dx \tag{33a}$$

$$v\left(x_0, \pm\frac{h}{2}\right) = \pm \frac{\beta}{\pi} \int_{-\infty}^{\infty} \frac{u\left(x, \pm\frac{h}{2}\right)}{x - x_0} \, dx \tag{33b}$$

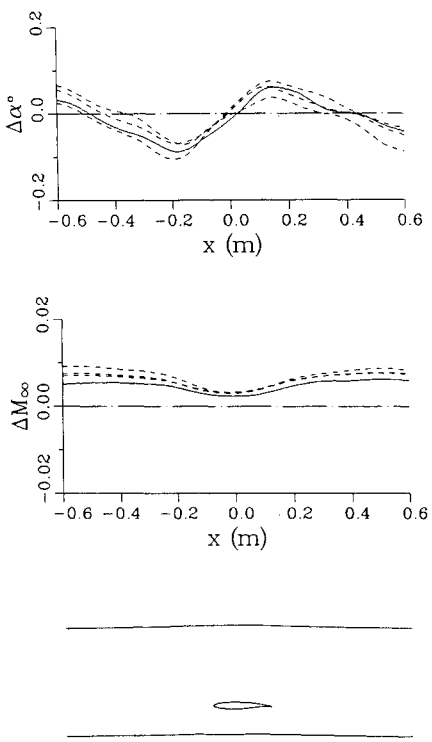

Fig. 4 Residual corrections evaluated by two-variable method for the 0.2-m chord CAST 7 airfoil in the 0.37-m × 0.39-m test section of ONERA T2, $M_\infty = 0.696$, $\alpha = 1.00$ deg, $C_N = 0.63$, $Rc = 5.9 \times 10^6$.

These "compressible-flow" versions of Hilbert's transforms, introduced by Sears[1] as functional relationships between two velocity components, define unconfined flow in a 2-D test section. We may note that in this special case the upper- and lower-boundary values are independent of one another (decoupling of infinite exterior regions). It is also important to remember that Eqs. (33) describe conjugate transforms, so that enforcement of either one ensures interference-free flow; see Appendix B.

C. Interface Discontinuity Method

This residual interference method, closely related to the two-variable method, utilizes exterior flow calculations. The general idea, as described by Sears and Erickson,[36] is essentially this: the flowfield is considered to consist of an experimental inner region joined at an interface to a computed outer region. If the computed outer flow satisfies the unconfined flow conditions and matches along the interface the inner flow, then the combined flowfield is continuous, representing unconfined flow around the model. The matching error, or discontinuity, provides a measure of the residual interference. It can be quantified by removing the discontinuity by a surface distribution of singularities. These singularities do not affect the unconfined flow condition in the outer region but do introduce velocity perturbations at the position of the test model, which can then be interpreted as the usual wall interference corrections.

As in the two-component method, Green's second identity will guide us to the appropriate singularities and their density functions. Considering the disturbance velocity potential $\tilde{\phi}$ of the fictitious flow in the exterior region, satisfying the far-field boundary condition

$$\nabla\tilde{\phi}(\boldsymbol{r}) \to 0 \quad \text{as} \quad |\boldsymbol{r}| \to \infty$$

then for an interior point $\boldsymbol{r}_0$ it follows that

$$0 = \int\int_S \left[\tilde{\phi}(\boldsymbol{r})\frac{\partial G(\boldsymbol{r}_0,\boldsymbol{r})}{\partial n} - G(\boldsymbol{r}_0,\boldsymbol{r})\frac{\partial\tilde{\phi}(\boldsymbol{r})}{\partial n}\right] \mathrm{d}S$$

Subtracting it from Eq. (16), we obtain the interior value of the wall interference potential in terms of the differences of the interior and exterior flow potentials and their normal derivatives along the interface:

$$\phi_w(\boldsymbol{r}_0) = \int\int_S \left\{[\phi(\boldsymbol{r}) - \tilde{\phi}(\boldsymbol{r})]\frac{\partial G(\boldsymbol{r}_0,\boldsymbol{r})}{\partial n} - \left[\frac{\partial\phi(\boldsymbol{r})}{\partial n} - \frac{\partial\tilde{\phi}(\boldsymbol{r})}{\partial n}\right] G(\boldsymbol{r}_0,\boldsymbol{r})\right\} \mathrm{d}S \tag{34}$$

Physically, the integral in Eq. (34) can be interpreted as a surface distribution of doublets

$$\frac{\partial G(\boldsymbol{r}_0,\boldsymbol{r})}{\partial n} \quad \text{with density} \quad [\phi(\boldsymbol{r}) - \tilde{\phi}(\boldsymbol{r})]$$

and a surface distribution of sources

$$G(\boldsymbol{r}_0,\boldsymbol{r}) \quad \text{with density} \quad -\left[\frac{\partial\phi(\boldsymbol{r})}{\partial n} - \frac{\partial\tilde{\phi}(\boldsymbol{r})}{\partial n}\right]$$

It should be stressed that the potential $\tilde{\phi}$ is obtained by solving an exterior flow problem (CFD), but ϕ_w is obtained by a simple surface integration, as in the two-variable method. A practical advantage of Eq. (34) over Eq. (16) is that the involved densities are small quantities so that the residual interference can be evaluated with a better accuracy. On the other hand, the result is biased by the exterior flow computation. The autocorrective property applies as for the two-variable method, and the proof will not be repeated here.

The exterior flow can be calculated as a solution of a Neumann problem, satisfying the boundary condition

$$\frac{\partial\tilde{\phi}(\boldsymbol{r})}{\partial n} = \frac{\partial\phi(\boldsymbol{r})}{\partial n}, \quad \boldsymbol{r} \in S \tag{35}$$

where $\partial\phi(\boldsymbol{r})/\partial n$ is the normal component of disturbance velocity on the interface. For a solid wall boundary, it is equal and opposite to the normal component of the freestream velocity. The integral in Eq. (34) then reduces to the distribution of doublets

$$\phi_w(\boldsymbol{r}_0) = \int\int_S [\phi(\boldsymbol{r}) - \tilde{\phi}(\boldsymbol{r})]\frac{\partial G(\boldsymbol{r}_0,\boldsymbol{r})}{\partial n} \mathrm{d}S \tag{36}$$

For a cylindrical interface the integration by parts in the streamwise direction yields

$$\phi_w(\boldsymbol{r}_0) = -\frac{\beta}{2}\int\int_S [C_p(\boldsymbol{r}) - \tilde{C}_p(\boldsymbol{r})]\Omega(\boldsymbol{r}_0,\boldsymbol{r}) \mathrm{d}S \tag{37}$$

where the term in square brackets is the discontinuity of the pressure coefficient across the boundary, and Ω is the vortex singularity, Eq. (17). Equation (37) shows that, in this case, wall interference is defined by the "loading" of the walls.[37]

Alternatively, the exterior flow can be calculated as a solution of a Dirichlet problem, satisfying the boundary condition

$$\tilde{\phi}(\boldsymbol{r}) = \phi(\boldsymbol{r}), \quad \boldsymbol{r} \in S \tag{38}$$

In this case the integral in Eq. (34) reduces to the distribution of sources[38]

$$\phi_w(\boldsymbol{r}_0) = -\int\int_S \left[\frac{\partial\phi(\boldsymbol{r})}{\partial n} - \frac{\partial\tilde{\phi}(\boldsymbol{r})}{\partial n}\right] G(\boldsymbol{r}_0,\boldsymbol{r}) \mathrm{d}S \tag{39}$$

Finally, if the walls are adjusted to satisfy the conditions (35) and (38) simultaneously (a perfect match), then, from Eq. (34)

$$\phi_w(\boldsymbol{r}_0) \equiv 0$$

indicating that the flow inside the test section is interference free. The conditions of flow tangency and equal pressures along the interface imply that the desired interface is a stream tube. This streamlining principle for an adaptive wall test section, introduced by Goodyer,[2] is, of course, quite general and not necessarily restricted to linear subsonic flow.

The Cauchy integral approach, applicable to 2-D flow, proceeds along similar lines. Considering the complex disturbance velocity $\tilde{w}$ of the fictitious flow, analytic in the exterior region and vanishing at infinity, then for an interior point z_0 it follows that

$$0 = \frac{1}{2\pi i}\int_C \frac{\tilde{w}(z)}{z - z_0} \mathrm{d}z$$

Subtracting this equation from Eq. (24), we obtain the integral

$$w_w(z_0) = \frac{1}{2\pi i}\int_C \frac{w(z) - \tilde{w}(z)}{z - z_0} \mathrm{d}z \tag{40}$$

which may again be evaluated as indicated in Appendix A.

If the normal component of disturbance velocity is continuous across the interface,

$$\tilde{q}_n(z) = q_n(z), \quad z \in C \tag{41}$$

then from Eqs. (27) and (28)

$$w_w(z_0) = \int_C [q_t(z) - \tilde{q}_t(z)] \frac{i}{2\pi(z_0 - z)} \, ds \tag{42}$$

The wall interference velocity is represented by a contour distribution of vortices, whose density is equal to the discontinuity of the tangential component of velocity.

Conversely, if the tangential component of disturbance velocity is continuous,

$$\tilde{q}_t(z) = q_t(z), \quad z \in C \tag{43}$$

then

$$w_w(z_0) = \int_C -[q_n(z) - \tilde{q}_n(z)] \frac{1}{2\pi(z_0 - z)} \, ds \tag{44}$$

The wall interference velocity is represented by a contour distribution of sources, whose density is equal and opposite to the discontinuity of the normal component of velocity.

As indicated earlier, schemes for calculating residual interferences and strategies of wall adaptation are closely interrelated. This can be best illustrated[39] on Judd's streamlining algorithm.[40]

This iterative procedure utilizes calculations of the fictitious external flow matching the normal velocity,

$$\tilde{v}_j = v_j$$

along the interface $y = \pm h/2$, which approximates the upper and lower walls of a 2-D test section. Index j indicates the iteration (wall-adjustment) step. The individual wall slope adjustment $v_{j+1} - v_j$ is required to provide the next computed value of the streamwise component, $\tilde{u}_{j+1}$, equal to the average of the measured value u_j and the computed value $\tilde{u}_j$:

$$\tilde{u}_{j+1} = \frac{1}{2}(u_j + \tilde{u}_j)$$

This condition is equivalent to

$$\tilde{u}_{j+1} - \tilde{u}_j = \frac{1}{2}(u_j - \tilde{u}_j) \tag{45}$$

The slope adjustment can be obtained explicitly, using the unconfined flow conditions for the velocity pair $\tilde{u}_j$ and v_j. From Eq. (33b)

$$v_j\left(x_0, \pm\frac{h}{2}\right) = \pm\frac{\beta}{\pi} \int_{-\infty}^{\infty} \frac{\tilde{u}_j\left(x, \pm\frac{h}{2}\right)}{x - x_0} \, dx \tag{46}$$

Applying Eq. (46) to the difference $v_{j+1} - v_j$ and substituting from Eq. (45), Judd's wall adaptation formula[40] is readily obtainable:

$$v_{j+1}\left(x_0, \pm\frac{h}{2}\right) - v_j\left(x_0, \pm\frac{h}{2}\right) = \pm\frac{\beta}{2\pi} \int_{-\infty}^{\infty} \frac{u_j\left(x, \pm\frac{h}{2}\right) - \tilde{u}_j\left(x, \pm\frac{h}{2}\right)}{x - x_0} \, dx \tag{47}$$

If

$$\tilde{u}_j\left(x, \pm\frac{h}{2}\right) = u_j\left(x, \pm\frac{h}{2}\right) \tag{48}$$

then

$$v_{j+1}\left(x_0, \pm\frac{h}{2}\right) = v_j\left(x_0, \pm\frac{h}{2}\right)$$

indicating that the iterative process has terminated. Substituting Eq. (48) in Eq. (46), we obtain the unconfined flow condition for the measured disturbance velocity components u_j and v_j, implying that the tunnel flow in the jth iteration is interference free.

III. Conclusion

The techniques reviewed in this paper are applicable provided that the potential flow equation can be linearized near the test section boundaries. The basic assumption is that the perturbations measured at or near the walls are separate contributions of perturbations due to the model and perturbations induced by the walls. In the averaged sense, flow near the walls is only slightly perturbed (small fluxes across ventilated walls, gradual changes of curvature of flexible walls, no stagnation points, etc.) so that linearization can be stretched up to much higher stream Mach numbers than is possible, for example, for flow in the vicinity of a wing.

For supercritical flow conditions at the walls, the principle of wall adaptation based on matching of the boundary values of the measured inner flow and computed outer flow remains valid. The adaptive wall concept serves then as a perfect example of a coupling of experimental and numerical methods: flow near the model, which is very complex, is investigated experimentally in the wind tunnel, whereas the outer flow, which is predominantly inviscid, is modeled on a computer.

However, assessment of residual interference from the discontinuity of the measured and computed boundary data can no longer be done by a linear method. One of the most innovative concepts in transonic wall interference has been given by Kemp,[41] and extended to the adaptive test section case by Green and Newman.[42] The method is based on matching of the pressure distribution measured on the model with that computed for an inviscid flow past an effective model at corrected freestream conditions. One solves two inviscid flow problems: 1) an inverse (design-like) problem, where pressure measurements on the walls and on the model are used as the boundary conditions to obtain the equivalent inviscid model shape, and 2) a direct problem where an unconfined flow past the obtained model shape is solved. The corrected stream Mach number and angle of attack are obtained iteratively, by matching the measured and calculated model data. A more detailed review of new developments and trends in this field is given in Ref. 43.

Appendix A

Approximating the counterclockwise-oriented contour C by line segments, the Cauchy-type integral

$$w_w(z_0) = \frac{1}{2\pi i} \int_C \frac{f(z)}{z - z_0} \, dz \tag{A1}$$

reduces to the sum

$$w_w(z_0) = \sum_j \Delta_j w_w(z_0) \tag{A2}$$

where

$$\Delta_j w_w(z_0) = \frac{1}{2\pi i} \int_{z_j}^{z_{j+1}} \frac{f(z)}{z - z_0} \, dz \tag{A3}$$

is the contribution of the jth segment.

Assuming a linear variation of the density function f be-

tween the segment end points z_j and z_{j+1}:

$$f(z) = f_j + \frac{f_{j+1}-f_j}{z_{j+1}-z_j}(z-z_j)$$

$$= \frac{f_{j+1}-f_j}{z_{j+1}-z_j}(z-z_0) + f_{j+1}\frac{z_0-z_j}{z_{j+1}-z_j} - f_j\frac{z_0-z_{j+1}}{z_{j+1}-z_j} \quad \text{(A4)}$$

and substituting it in Eq. (A3), we find that[44]

$$\Delta_j w_w(z_0) = \frac{f_{j+1}-f_j}{2\pi i} + \frac{1}{2\pi i}\left[f_{j+1}\frac{z_0-z_j}{z_{j+1}-z_j} - f_j\frac{z_0-z_{j+1}}{z_{j+1}-z_j}\right] \ell n \frac{z_{j+1}-z_0}{z_j-z_0} \quad \text{(A5)}$$

In the limit as the point z_0 approaches an interior point of the jth segment from the left (test section side)

$$\ell n \frac{z_{j+1}-z_0}{z_j-z_0} \to \ell n \left|\frac{z_{j+1}-z_0}{z_j-z_0}\right| + i\pi$$

complying with Eq. (29)

Appendix B

Supposing that Eq. (33a) holds true, we can evaluate the right-hand side of Eq. (33b) using the Poincaré-Bertrand transposition formula[17]:

$$\pm\frac{\beta}{\pi}\int_{-\infty}^{\infty}\frac{u\left(x,\pm\frac{h}{2}\right)}{x-x_0}\,dx$$

$$= \pm\frac{\beta}{\pi}\int_{-\infty}^{\infty}\frac{dx}{x-x_0}\left(\mp\frac{1}{\beta\pi}\int_{-\infty}^{\infty}\frac{v\left(\xi,\pm\frac{h}{2}\right)}{\xi-x}\,d\xi\right)$$

$$= \frac{1}{\pi i}\int_{-\infty}^{\infty}\frac{dx}{x-x_0}\left(\frac{1}{\pi i}\int_{-\infty}^{\infty}\frac{v\left(\xi,\pm\frac{h}{2}\right)}{\xi-x}\,d\xi\right)$$

$$= v\left(x_0,\pm\frac{h}{2}\right) + \frac{1}{\pi i}\int_{-\infty}^{\infty} v\left(\xi,\pm\frac{h}{2}\right)d\xi \left(\frac{1}{\pi i}\int_{-\infty}^{\infty}\frac{dx}{(x-x_0)(\xi-x)}\right)$$

Since the last integral vanishes,

$$\int_{-\infty}^{\infty}\frac{dx}{(x-x_0)(\xi-x)} = \frac{1}{\xi-x_0}\left(\int_{-\infty}^{\infty}\frac{dx}{x-x_0} - \int_{-\infty}^{\infty}\frac{dx}{x-\xi}\right) = 0$$

the validity of Eq. (33b) is established.

Acknowledgment

The TCT and T2 wind-tunnel data were made available to NAE through a collaborative NASA/NAE Transonic Wall Interference Research Program and the participation in the AGARD FDP Working Group 12 on Adaptive Wind Tunnels.

References

[1]Sears, W. R., "Self Correcting Wind Tunnels," *The Aeronautical Journal*, Vol. 78, March 1974, pp. 80–89.

[2]Goodyer, M. J., "The Self Streamlining Wind Tunnel," NASA TMX-72699, Aug. 1975.

[3]Wedemeyer, E., "Wind Tunnel Testing of Three Dimensional Models in Wind Tunnels with Two Adaptive Walls," Von Kármán Institute for Fluid Dynamics, Belgium, TN-147, Sept. 1982.

[4]Lamarche, L., "Reduction of Wall Interference for Three Dimensional Models with Two Dimensional Wall Adaptation," Ph.D. Thesis, Université Libre de Bruxelles, 1986.

[5]Wedemeyer, E., and Lamarche, L., "The Use of 2-D Adaptive Wall Test Sections for 3-D Flows," *Proceedings of the AIAA 15th Aerodynamic Testing Conference*, AIAA, Washington, DC, May 1988, pp. 363–371.

[6]Kraft, E. M., Ritter, A., and Laster, M. L., "Advances at AEDC in Treating Transonic Wind Tunnel Wall Interference," *ICAS Proceedings 1986*, pp. 748–769.

[7]Smith, J., "Measured Boundary Conditions Methods for 2D Flow," AGARD-CP-335, May 1982, pp. 9.1–9.15.

[8]Schairer, T. E., "Two-Dimensional Wind-Tunnel Interference from Measurements on Two Contours," *Journal of Aircraft*, Vol. 21, June 1984, pp. 414–419.

[9]Baldwin, B. S., Turner, J. B., and Knechtel, E. D., "Wall Interference in Wind Tunnels With Slotted and Porous Boundaries at Subsonic Speeds," NACA TN-3176, 1954.

[10]Garner, H. C., Rogers, E. W. E., Acum, W. E. A., and Maskell, E. C., "Subsonic Wind Tunnel Wall Corrections," AGARD-109, Oct. 1966, pp. 389–390.

[11]Capelier, C., Chevalier, J. P., and Bouniol, F., "Nouvelle Méthode de Correction des Effets de Parois en Courant Plan," *La Recherche Aérospatiale*, Jan.–Feb. 1978, pp. 1–11.

[12]Stakgold, I., *Boundary Value Problems of Mathematical Physics*, Vol. 2, Macmillan, New York, 1968, pp. 122–123.

[13]Mokry, M., Digney, J. R., and Poole, R. J. D., "Doublet-Panel Method for Half-Model Wind-Tunnel Corrections," *Journal of Aircraft*, Vol. 24, May 1987, pp. 322–327.

[14]Mokry, M., and Ohman, L. H., "Application of the Fast Fourier Transform to Two-Dimensional Wind Tunnel Wall Interference," *Journal of Aircraft*, Vol. 17, June 1980, pp. 402–408.

[15]Mokry, M., "Subsonic Wall Interference Corrections for Finite-Length Test Sections Using Boundary Pressure Measurements," AGARD-CP-335, May 1982, pp. 10.1–10.15.

[16]Rizk, M. H., and Smithmeyer, M. G., "Wind-Tunnel Interference Corrections for Three-Dimensional Flows," *Journal of Aircraft*, Vol. 19, June 1982, pp. 465–472.

[17]Gakhov, F. D., *Boundary Value Problems*, Pergamon, 1966, pp. 50, 208–209.

[18]Chevallier, J. P., "Survey of ONERA Activities on Adaptive-Wall Applications and Computation of Residual Corrections," *Wind Tunnel Wall Interference Assessment/Correction 1983*, NASA CP-2319, 1984, pp. 43–58.

[19]GARTEUR Action Group AD (AG-02), "Two-Dimensional Transonic Testing Methods," National Aerospace Laboratory, the Netherlands, TR-83086 U, July 1981.

[20]Archambaud, J. P., and Chevallier, J. P., "Utilisation de Parois Adaptables pour les Essais en Courant Plan," AGARD CP-335, May 1982, pp. 14.1–14.14.

[21]Paquet, J. B., "Perturbations Induites par les Parois d'une Soufflerie—Méthodes Intégrales," Thèse Ing. Doc., Université de Lille, 1979.

[22]Lo, C. F., "Tunnel Interference Assessment by Boundary Measurements," *AIAA Journal*, Vol. 16, April 1978, pp. 411–413.

[23]Lo, C. F., and Kraft, E. M., "Convergence of the Adaptive-Wall Wind Tunnel," *AIAA Journal*, Vol. 16, Jan. 1978, pp. 67–72.

[24]Kraft, E. M., and Dahm, W. J. A., "Direct Assessment of Wall Interference in a Two-Dimensional Subsonic Wind Tunnel," AIAA Paper 82-0187, Jan. 1982.

[25]Amecke, J., "Direkte Berechnung von Wandinterferenzen und Wandadaptation bei zweidimensionaler Strömung in Windkanälen mit geschlossenen Wänden," Deutsche Forschungs und Versuchsanstatt für Luft und Raumfahrt FB 85-62, Nov. 1985; also NASA TM-88523, Dec. 1986.

[26]Ashill, P. R., and Weeks, D. J., "A Method for Determining Wall-Interference Corrections in Solid-Wall Tunnels from Measurements of Static Pressure at the Walls," AGARD CP-335, May 1982, pp. 1.1–1.12.

[27]Ashill, P. R., and Keating, R. F. A., "Calculation of Tunnel Wall Interference from Wall-Pressure Measurements," *Journal of the Royal Aeronautical Society*, Jan. 1988, pp. 36–53.

[28]Barche, J., "Zur Ermittlung von Wandinterferenzen," *Zeitschrift für Flugwisensschaften und Weltraumforschung*, Vol. 4, 1980, pp. 389–396.

[29]Labrujère, T. E., "Correction for Wall-Interference by Means of a Measured-Boundary-Condition Method," National Aerospace Laboratory, TR 84114 U, the Netherlands, Nov. 1984.

[30]Maarsingh, R. A., Labrujère, T. E., and Smith, J., "Accuracy of Various Wall-Correction Methods for 3D Subsonic Wind Tunnel Testing," AGARD CP-429, Sept. 1987, pp. 17.1–17.13.

[31]Mineck, R. E., "Wall Interference Tests of a CAST 10-2/DOA 2 Airfoil in an Adaptive-Wall Test Section," Supplement to NASA TM-4015, Dec. 1987.

[32]Niederdrenk, P., and Wedemeyer, E., "Analytic Near-Field Boundary Condition for Transonic Flow Computations," *AIAA Journal*, Vol. 25, June 1987, pp. 884–886.

[33]Lo, C. F., and Sickles, W. L., "Analytic and Numerical Investigation of the Convergence for the Adaptive-Wall Concept," AEDC TR-79-55, Nov. 1979.

[34]Archambaud, J. P., Mignosi, A., and Seraudie, A., "Rapport d'Essais sur Profil CAST 7 Effectués à la Soufflerie T2 en Présence de Parois Auto-Adaptables en Liaison avec le Groupe GARTEUR AD (AG02)," Rapport Technique 24/3075, ONERA CERT, Aug. 1982.

[35]Archambaud, J. P., and Mignosi, A., "Two-Dimensional and Three-Dimensional Adaptation at the T2 Transonic Wind Tunnel of ONERA/CERT," *Proceedings of the AIAA 15th Aerodynamic Testing Conference*, AIAA, Washington, DC, May 1988, pp. 342–350.

[36]Sears, W. R., and Erickson, J. C., Jr., "Adaptive Wind Tunnels," *Annual Review of Fluid Mechanics*, Vol. 20, 1988, pp. 17–34.

[37]Goodyer, M. J., and Wolf, S. W. D., "The Development of a Self Streamlining Flexible Walled Transonic Test Section," *AIAA Journal*, Vol. 20, Feb. 1982, pp. 227–234.

[38]Rebstock, R., and Lee E. E., Jr., "Capabilities of Wind Tunnels With Two Adaptive Walls to Minimize Boundary Interference in 3-D Model Testing," NASA CP-3020, Vol. 1, Part 2, 1989, pp. 891–910.

[39]Russo, G. P., and Zuppardi, G., "Numerical Simulation of an Adaptive Wall Wind Tunnel: A Comparison of Two Different Strategies," L'aerotecnica, Missili e Spazio, Vol. 66, No. 4, 1987, pp. 239–249.

[40]Judd, M., Wolf, S. W. D., and Goodyer, M. J., "Analytical Work in Support of the Design and Operation of Two Dimensional Self Streamlining Test Sections," NASA CR-145019, 1976.

[41]Kemp, W. B., Jr., "Toward the Correctable-Interference Transonic Wind Tunnel," *Proceedings of the AIAA 9th Aerodynamic Testing Conference*, AIAA New York, 1976, pp. 31–38.

[42]Green, L. L., and Newman, P. A., "Transonic Wall Interference Assessment and Corrections for Airfoil Data from the 0.3-Meter TCT Adaptive Wall Test Section," AIAA Paper 87-1431, June 1987.

[43]Newman, P. A., Kemp, W. B., Jr., and Garriz, J. A., "Emerging Technology for Transonic Wind-Tunnel-Wall Interference Assessment and Corrections," Society of Automotive Engineers 881454, Oct. 1988.

[44]Hromadka, T. V., II, *The Complex Variable Boundary Element Method*, Springer-Verlag, Berlin, 1984, pp. 53–55.